

Intracellular regulation of cell signaling cascades: how location makes a difference

Yongyun Hwang, Praveen Kumar & Abdul I. Barakat

Journal of Mathematical Biology

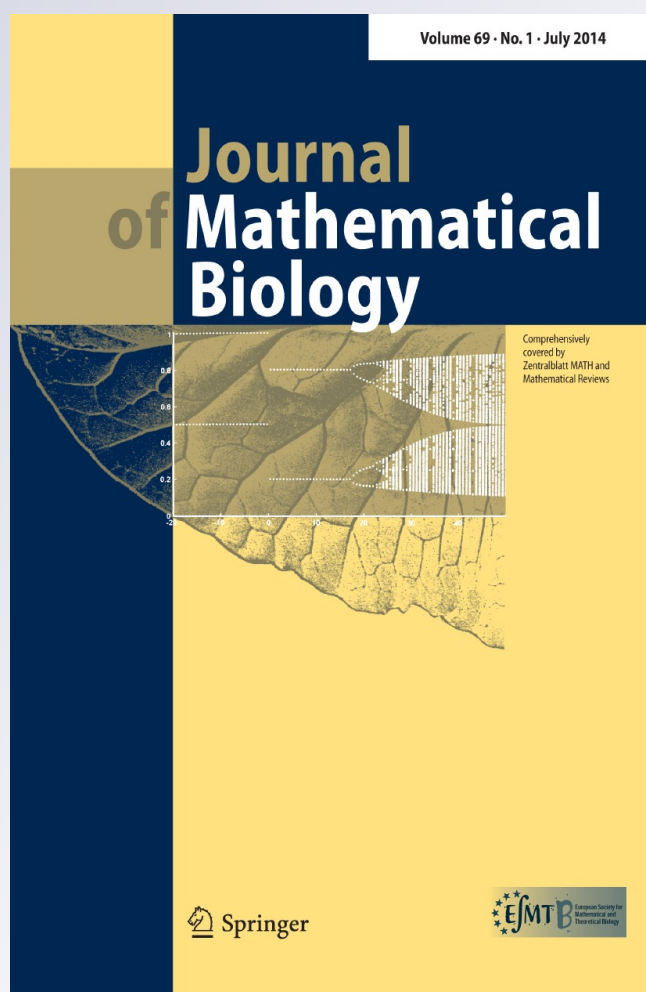
ISSN 0303-6812

Volume 69

Number 1

J. Math. Biol. (2014) 69:213-242

DOI 10.1007/s00285-013-0701-7



Your article is protected by copyright and all rights are held exclusively by Springer-Verlag Berlin Heidelberg. This e-offprint is for personal use only and shall not be self-archived in electronic repositories. If you wish to self-archive your article, please use the accepted manuscript version for posting on your own website. You may further deposit the accepted manuscript version in any repository, provided it is only made publicly available 12 months after official publication or later and provided acknowledgement is given to the original source of publication and a link is inserted to the published article on Springer's website. The link must be accompanied by the following text: "The final publication is available at link.springer.com".

Intracellular regulation of cell signaling cascades: how location makes a difference

Yongyun Hwang · Praveen Kumar ·
Abdul I. Barakat

Received: 24 August 2012 / Revised: 1 June 2013 / Published online: 18 June 2013
© Springer-Verlag Berlin Heidelberg 2013

Abstract Organelles such as endosomes and the Golgi apparatus play a critical role in regulating signal transmission to the nucleus. Recent experiments have shown that appropriate positioning of these organelles within the intracellular space is critical for effective signal regulation. To understand the mechanism behind this observation, we consider a reaction-diffusion model of an intracellular signaling cascade and investigate the effect on the signaling of intracellular regulation in the form of a small release of phosphorylated signaling protein, kinase, and/or phosphatase. Variational analysis is applied to characterize the most effective regions for the localization of this intracellular regulation. The results demonstrate that signals reaching the nucleus are most effectively regulated by localizing the release of phosphorylated substrate protein and kinase near the nucleus. Phosphatase release, on the other hand, is nearly equally effective throughout the intracellular space. The effectiveness of the intracellular regulation is affected strongly by the characteristics of signal propagation through the cascade. For signals that are amplified as they propagate through the cascade, reactions in the upstream levels of the cascade exhibit much larger sensitivities to regulation by release of phosphorylated substrate protein and kinase than downstream reactions. On the other hand, for signals that decay through the cascade, downstream reactions exhibit larger sensitivity than upstream reactions. For regulation by phosphatase release,

Y. Hwang (✉) · A. I. Barakat
Hydrodynamics Laboratory (LadHyX), Ecole Polytechnique, Palaiseau, France
e-mail: yongyun@ladhyx.polytechnique.fr

Present address:

Y. Hwang
Department of Applied Mathematics and Theoretical Physics (DAMTP),
University of Cambridge, Cambridge, UK
e-mail: Y.Hwang@damtp.cam.ac.uk

P. Kumar
Aerospace Engineering, Indian Institute of Technology, Kharagpur, India

all reactions within the cascade show large sensitivity for amplified signals but lose this sensitivity for decaying signals. We use the analysis to develop a simple model of endosome-mediated regulation of cell signaling. The results demonstrate that signal regulation by the modeled endosome is most effective when the endosome is positioned in the vicinity of the nucleus. The present findings may explain at least in part why endosomes in many cell types localize near the nucleus.

Keywords Cell signaling · MAP kinase · Sensitivity analysis · Adjoint variables · Endocytosis

Mathematics Subject Classification 92B05 Biomathematics · 65K10 Optimization and variational techniques

1 Introduction

Signaling cascades through covalent protein modification cycles play an important role in regulating cell proliferation, mitosis, differentiation, and apoptosis. The covalent protein modification cycle often consists of two interconvertible enzyme-mediated reactions: phosphorylation and dephosphorylation. The phosphorylation of substrate proteins in the cytoplasm is often initiated by signaling complexes at the cell membrane. The signal carried by a particular phosphorylated protein is transferred down the cascade to the protein modification cycle at the next level by phosphorylating the related substrate protein. Typically, biochemical signals, which are activated at the cell membrane by external stimuli such as growth factors and/or mechanical forces, undergo a cascade of multiple protein modification cycles before attaining the nucleus where gene expression is regulated. Examples of such cascades are the MAPK (mitogen-activated-protein kinase) (Chang and Karin 2001) and small GTPase cascades (Takai et al. 2001).

A number of previous studies have described mathematical models of intracellular signaling. In this context, both static and dynamic responses of cascades of single and multiple protein modification cycles have been investigated (Tyson et al. 2003; Kholodenko 2006, 2010). The models have demonstrated that in the case of single protein modification cycles, the steady-state response of phosphorylated (active) signaling proteins is exquisitely sensitive to the concentration of phosphorylating and dephosphorylating enzymes, particularly when the reaction is close to saturation (Stadtman and Chock 1977; Goldbeter and Koshland 1981). This behavior, often referred to as ultrasensitivity, becomes even more pronounced in cascades of multiple protein modification cycles (Goldbeter and Koshland 1981; Ferrell 1997). Importantly, it has been found that the networking topology of multiple protein modification cycle cascades plays a crucial role in generating a wide variety of temporally-dependent output signaling patterns. For instance, positive and/or negative feedback looping among the reaction partners may generate different possible signaling outputs such as sustained, transient (Brightman and Fell 2000; Asthagiri and Lauffenburger 2001), bistable (Bhalla et al. 2002; Xiong and Ferrell 2003), or oscillatory responses (Nakayama et al. 2008), which may have different effects on gene expression patterns at the nucleus. Further

details on the diversity of possible temporal responses may be found in recent reviews (Tyson et al. 2003; Kholodenko 2006, 2010).

Most previous modeling studies have assumed that signaling proteins and related enzymes are uniformly distributed within the intracellular space (i.e. no spatial dependence), although the notion of 'space' has been introduced fairly recently into theoretical descriptions of signaling cascades. The spatially inhomogeneous distribution of cell signal intensity stems essentially from the fact that the two enzymes involved in each protein modification cycle are often present at different intracellular locations (Brown and Kholodenko 1999; Kholodenko 2002, 2006, 2010; Munoz-Garcia et al. 2010). For example, phosphorylating enzymes such as kinases and GEF (guanine nucleotide exchange factors) are often localized exclusively at the plasma membrane, whereas dephosphorylating enzymes such as phosphatases and GAP (GTPase-activating protein) appear to be uniformly distributed throughout the cytoplasm. Therefore, many cell signals are initiated by phosphorylation at the cell membrane. As these signals propagate towards the nucleus, they are partially inactivated due to the dephosphorylating enzymes in the cytoplasm. This mechanism leads to formation of a concentration gradient of the phosphorylated signaling proteins with the characteristic length scale,

$$\xi = \sqrt{\frac{D}{k_i}}, \quad (1)$$

where k_i ($\simeq 5 \text{ sec}^{-1}$) is the rate constant for dephosphorylation and D ($\simeq 5 \times 10^{-12} \text{ m}^2 \text{ sec}^{-1}$) is the diffusion coefficient of the phosphorylated signaling protein (Kholodenko 2006). The presence of a concentration gradient of phosphorylated substrate proteins was predicted in previous theoretical studies (Brown and Kholodenko 1999) and has been experimentally confirmed for the small GTPase Ran (Kalab et al. 2002), the microtubule-binding protein stathmin (Niethammer et al. 2004), and the yeast MAPK Fus3 (Maeder et al. 2007). Theoretical predictions have shown that the concentration gradient of the phosphorylated proteins may be very steep as typical values of k_i and D lead to $\xi \sim O(1 \mu\text{m})$. Given that the length scale of many eukaryotic cells is $O(10 \mu\text{m})$, the small value of ξ suggests the likely existence of several mechanisms which facilitate signal transmission to distant intracellular sites (Brown and Kholodenko 1999; Kholodenko 2002, 2006).

Trafficking of intracellular signaling complexes by molecular motors along the cytoskeleton is thought to constitute an important mechanism for signal transmission to distant intracellular sites (Flore and Camilli 2001; Kholodenko 2002, 2003; Perlson et al. 2005; Miaczynska et al. 2004; Howe and Mobley 2004; Birtwistle and Kholodenko 2009; Sadowski et al. 2009). The endosome is an example of such a signaling complex. Endocytosis was traditionally believed to be a signal attenuation mechanism (Koenig and Edwardson 1997). However, a number of recent studies have shown that it also plays an important role in signal transduction (Kholodenko 2002, 2006; Howe and Mobley 2004; Birtwistle and Kholodenko 2009; Sadowski et al. 2009): for instance, in COS-7 cells, when endocytosis is inhibited, ERK (extracellular signal-regulated kinase) activation is impaired (Pierce and Maudsley 2000). More importantly, the spatial localization of endosomes within cells appears to be critical for signal regulation (Hoepfner et al. 2005; Taub et al. 2007). In most cells, endosomes

localize preferentially near the nucleus (Burkhardt et al. 1997; Harada et al. 1998). A recent study has demonstrated that relocating late endosomes to the cell periphery significantly disturbs MAPK signaling in response to epidermal growth factor (Taub et al. 2007). This finding suggests that the proper intracellular positioning of signaling complexes is essential for signal transduction. In addition to endosomes, other types of intracellular signal complexes, for example the Golgi apparatus (Bivona et al. 2003) and nuclear-outer-membrane bound proteins (Warren et al. 2010), are often located near their target sites (periphery of the nucleus) (Burkhardt et al. 1997; Harada et al. 1998). Although spatial proximity of intracellular signaling complexes to their target sites may appear intuitively advantageous, an understanding of the physical factors that contribute to this advantage remains lacking.

The objective of the present study is to gain insight into how the localization of a given intracellular signaling complex affects signal transduction. To this end, we consider a conceptual reaction-diffusion model for signaling cascades (Munoz-Garcia et al. 2009) and use variational analysis to investigate the sensitivity of intracellular signaling to the release of a small amount of phosphorylated signaling protein, kinase, and/or phosphatase at various locations within the intracellular space. We then discuss the physical mechanisms that determine how intracellular localization affects the signal reaching its target site and conclude with a simple model for the potential role of endocytosis in intracellular signaling.

2 Model analysis

2.1 Model of a signaling cascade

Following Munoz-Garcia et al. (2009), we consider a model of a signaling cascade as depicted in Fig. 1. The model consists of a cascade of multiple protein modification cycles, where both phosphorylated and unphosphorylated forms of substrate proteins are considered. Consistent with experimental observations and previous mathematical models (Kholodenko 2006, 2010), we assume that the initial kinase in the cascade, which catalyzes phosphorylation of substrate proteins at the first level of the cascade ($n = 1$), is positioned exclusively at the cell membrane. At each level in the signaling cascade, phosphorylated proteins are dephosphorylated by a phosphatase which is assumed to be uniformly distributed throughout the cytoplasm. The model assumes that there is no signaling feedback of any type although some signaling cascades exhibit upregulation of phosphatase activity through a negative feedback loop when signaling is activated (Brightman and Fell 2000). Finally, we assume that the phosphatase we consider is not very specific to any signaling molecules. It is recognized that this assumption is not strictly valid: for example, in the MAP kinase cascade, a phosphatase may be very specific to the MAPKKK in the cascade. However, we believe that this assumption is reasonable for illustrating the general behavior.

For simplicity, we neglect curvature effects as in Munoz-Garcia et al. (2009) and consider one-dimensional intracellular space, $x \in [0, L]$, where $x = 0$ and $x = L$ are the cell membrane (where signaling originates) and the nucleus (signal target site), respectively. We assume that protein synthesis and degradation are negligible on the time scale of interest and that all proteins throughout the signaling cascade have

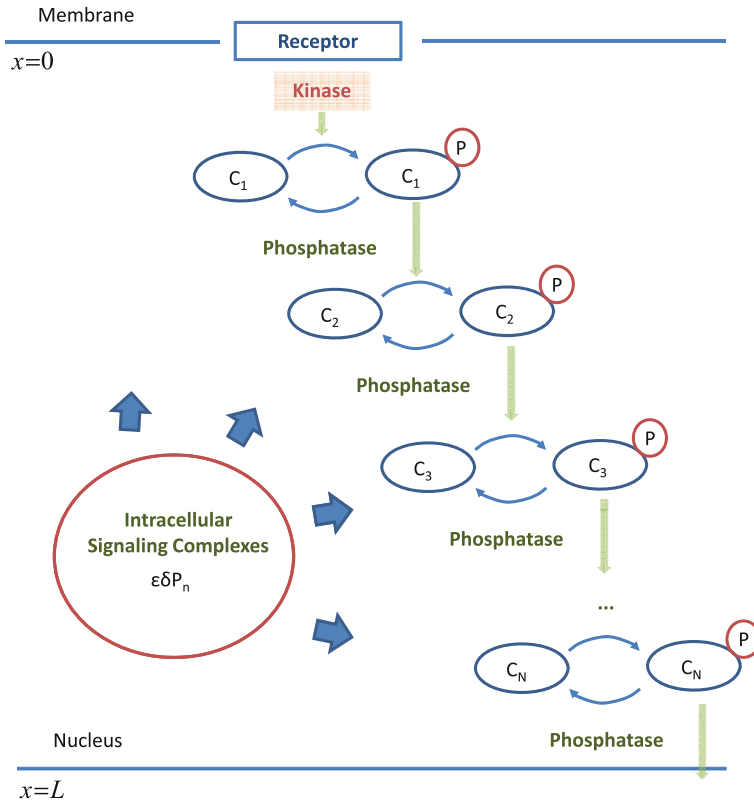


Fig. 1 Schematic diagram of a signaling cascade in the present study

the same diffusivity (D) (for the effect of different diffusivities of phosphorylated and dephosphorylated proteins, the reader is referred to [Stelling and Kholodenko \(2009\)](#)). These assumptions allow us to set the total concentration of phosphorylated (active) and unphosphorylated (inactive) protein at each cascade level as constant in time t ([Stelling and Kholodenko 2009](#)), i.e. $C_n^{tot} = \bar{C}_n(x, t) + C_n(x, t)$, where $C_n(x, t)$ and $\bar{C}_n(x, t)$ respectively denote the concentrations of phosphorylated and unphosphorylated signaling proteins at cascade level n . For convenience, we normalize the concentrations by C_n^{tot} : $c_n(x, t) = C_n(x, t)/C_n^{tot}$ and $\bar{c}_n(x, t) = \bar{C}_n(x, t)/C_n^{tot}$, leading to the following relation:

$$\bar{c}_n(x, t) + c_n(x, t) = 1. \tag{2}$$

In terms of the normalized concentrations, the reaction-diffusion equations for the phosphorylated species in the cascade in [Fig. 1](#) can be written as follows (see [Appendix A](#) for further details on the normalization):

$$\begin{aligned} \frac{\partial c_1}{\partial t} &= D \frac{\partial^2 c_1}{\partial x^2} - v_1^{phos} + \epsilon \delta p_1(x, t), \\ \frac{\partial c_n}{\partial t} &= D \frac{\partial^2 c_n}{\partial x^2} + v_n^{kin} - v_n^{phos} + \epsilon \delta p_n(x, t) \quad \text{for } n = 2, 3, \dots, N. \end{aligned} \tag{3a}$$

with boundary conditions,

$$\begin{aligned}
 D \frac{\partial c_1}{\partial x} \Big|_{x=0} &= -v_1^{kin}, \quad \frac{\partial c_1}{\partial x} \Big|_{x=L} = 0, \\
 \frac{\partial c_n}{\partial x} \Big|_{x=0} &= \frac{\partial c_n}{\partial x} \Big|_{x=L} = 0 \quad \text{for } n = 2, 3, \dots, N.
 \end{aligned}
 \tag{3b}$$

Here, v_n^{kin} and v_n^{phos} are respectively the reaction rates of phosphorylation and dephosphorylation of the substrate protein. For these processes, we consider Michaelis-Menten kinetics as done elsewhere (Kholodenko 2006; Munoz-Garcia et al. 2009) so that:

$$\begin{aligned}
 v_1^{kin} &= k_1^a \frac{1 - c_1}{1 + \frac{1-c_1}{m_1^a}} \Big|_{x=0}, \quad v_n^{kin} = k_n^a \frac{c_{n-1}(1 - c_n)}{1 + \frac{1-c_n}{m_n^a}} \quad \text{for } n = 2, 3, \dots, N, \\
 v_n^{phos} &= k_n^i \frac{c_n}{1 + \frac{c_n}{m_n^i}} \quad \text{for } n = 1, 2, \dots, N,
 \end{aligned}
 \tag{4}$$

where k_n^a and k_n^i are the apparent first-order rate constants for the linear kinetic domain of the kinase and phosphatase reactions, and m_n^a and m_n^i are dimensionless (normalized) Michaelis constants that represent the extent of saturation of each enzyme kinetics. If m_n^a or m_n^i is much smaller than $O(1)$, then the corresponding reaction is close to saturation. On the other hand, if either of these two parameters is much larger than $O(1)$, then the corresponding reaction is far from saturation. We note that the dimensions of the first-order rate constant at the membrane (k_1^a) differ from those of the rate constants in the cytoplasm ($m \text{ sec}^{-1}$ for k_1^a vs. sec^{-1} for k_n^a).

In Eq. (3a, 3b), we introduce an external driving (or source) term $\delta p_n(x, t)$ with small amplitude ϵ at all cascade levels. This term simulates the addition of new intracellular signaling complexes or perturbation in existing complexes. Depending on the intracellular signaling complex of interest, it is possible to formulate a specific model for $\delta p_{n,j}(x, t)$ as done for endosomes in the last section of the present work. In general, the form that $\delta p_{n,j}(x, t)$ takes will depend on the reaction involved in the signaling complexes and their scaffolds. Because the goal of the present study is to gain broad insight into intracellular signal regulation, we introduce a fairly general form of this source term where $\delta p_n(x, t)$ represents the release of a small amount of phosphorylated signaling protein, kinase, and phosphatase at each level n of the signaling cascade. Thus, $\delta p_n(x, t)$ may be written as follows:

$$\delta p_n(x, t) = (\delta f_n + \delta v_n^p - \delta v_n^c) \delta(x - x_l),
 \tag{5a}$$

where x_l is the spatial location at which the source term is positioned and $\delta(x)$ is the Dirac delta function. Here, δf_n is the release rate of the phosphorylated signaling protein at level n , δv_n^p is the production rate by the added kinase at level n , and δv_n^c is the consumption rate by the added phosphatase at level n . As in the reaction terms of each protein modification cycle, we also consider Michaelis-Menten kinetics for δv_n^p

and δv_n^c so that:

$$\delta v_n^p = \delta k_n^a \frac{1 - c_n}{1 + \frac{1 - c_n}{m_n^a}}, \quad \delta v_n^c = \delta k_n^i \frac{c_n}{1 + \frac{c_n}{m_n^i}}, \tag{5b}$$

where δk_n^a and δk_n^i are first-order rate constants for the linear kinetic domain. It should be pointed out that these rate constants have the same dimensions as the reaction constant k_1^a at the membrane, i.e. m sec^{-1} for both δk_n^a and δk_n^i .

2.2 Variational analysis

We wish to characterize the effect of the intracellular signal source term $\delta p_n(x, t)$ on the signal reaching the nucleus. To this end, we use variational analysis. We particularly wish to explore how the spatial location of $\delta p_n(x, t)$ within the intracellular space affects signaling at the nucleus. For simplicity, we limit the analysis to the steady case (i.e. $\partial c_n / \partial t = 0$). We also assume that only the phosphorylated protein species at the final level of the cascade ($n = N$) is involved in regulating the signal at the nucleus and that only the concentration of this species at the nucleus ($c_N|_{x=L}$) is important for this regulation. If the effect of the added source is sufficiently small ($\epsilon \ll 1$), then the change in $c_N|_{x=L}$ can be written as follows:

$$c_N|_{x=L} \rightarrow c_N|_{x=L} + \epsilon \delta c_N|_{x=L} + O(\epsilon^2), \tag{6}$$

where $\delta c_N|_{x=L}$ is the leading-order variation of $c_N|_{x=L}$ due to $\delta p_n(x)$ in Eq. (4). This leading-order variation is computed using the adjoint-based method (Gunzburger 2003), which has been widely used in optimal control theories. Since we introduced a small amount of the driving term $\epsilon \delta p_n(x)$ ($\epsilon \ll 1$), the resulting change of the solution of Eq. (4) is given as follows:

$$c_n(x) \rightarrow c_n(x) + \epsilon \delta c_n(x) + O(\epsilon^2), \tag{7}$$

where $c_n(x)$ is the solution of Eq. (4) without any driving term (i.e. $\epsilon = 0$), and $\epsilon \delta c_n(x)$ represents the change of the solution due to the driving term $\epsilon p_n(x)$. We substitute (7) into (3) and truncate it at $O(\epsilon)$. Then, the following equation for $\delta c_n(x)$ is obtained:

$$\underbrace{\begin{pmatrix} D \frac{\partial^2}{\partial x^2} + \alpha_1 & 0 & 0 & \dots & 0 \\ \beta_2 & D \frac{\partial^2}{\partial x^2} + \alpha_2 & 0 & \dots & 0 \\ 0 & \beta_3 & D \frac{\partial^2}{\partial x^2} + \alpha_3 & \dots & 0 \\ \vdots & \vdots & \ddots & \ddots & \vdots \\ 0 & 0 & \dots & \beta_N & D \frac{\partial^2}{\partial x^2} + \alpha_N \end{pmatrix}}_L \underbrace{\begin{pmatrix} \delta c_1 \\ \delta c_2 \\ \delta c_3 \\ \vdots \\ \delta c_N \end{pmatrix}}_{\delta c} + \underbrace{\begin{pmatrix} \delta p_1 \\ \delta p_2 \\ \delta p_3 \\ \vdots \\ \delta p_N \end{pmatrix}}_{\delta p} = 0, \tag{8}$$

with boundary conditions

$$D \frac{\partial \delta c_1}{\partial x} \Big|_{x=0} + \beta_1 \delta c_1 \Big|_{x=0} = 0, \quad \frac{\partial \delta c_1}{\partial x} \Big|_{x=L} = 0,$$

$$\frac{\partial \delta c_n}{\partial x} \Big|_{x=0} = \frac{\partial \delta c_n}{\partial x} \Big|_{x=L} = 0 \text{ for } n = 2, 3, \dots, N,$$

where the coefficients α_n and β_n are given as

$$\alpha_1 = -\frac{k_1^i}{1 + \frac{c_1}{m_1^i}} + \frac{k_1^i c_1}{m_1^i \left(1 + \frac{c_1}{m_1^i}\right)^2},$$

$$\alpha_n = -\frac{k_n^i}{1 + \frac{c_n}{m_n^i}} + \frac{k_n^i c_n}{m_n^i \left(1 + \frac{c_n}{m_n^i}\right)^2} - \frac{k_n^a c_{n-1}}{1 + \frac{1-c_n}{m_n^a}}$$

$$+ \frac{k_n^a (1 - c_n) c_{n-1}}{m_n^a \left(1 + \frac{1-c_n}{m_n^a}\right)^2} \text{ for } n = 2, 3, \dots, N, \tag{9}$$

$$\beta_1 = -\left(\frac{k_1^a}{1 + \frac{1-c_1}{m_1^a}} - \frac{k_1^a (1 - c_1)}{m_1^a \left(1 + \frac{1-c_1}{m_1^a}\right)^2} \right) \Big|_{x=0}, \beta_n$$

$$= -\frac{k_n^a (1 - c_n)}{1 + \frac{1-c_n}{m_n^a}} \text{ for } n = 2, 3, \dots, N.$$

Here, α_n and β_n are functions of only $c_n(x)$, indicating that Eq. (8) is linear.

Now, we extract $\delta c_N \Big|_{x=L}$ using the linear nature of Eq. (8). It is useful to introduce the following standard inner product for vector variables such as δc , δp , and so on:

$$\langle \mathbf{f}, \mathbf{g} \rangle = \int_0^L \mathbf{f}^T \mathbf{g} \, dx, \tag{10}$$

where $\mathbf{f} = [f_1 \ f_2 \ f_3 \ \dots \ f_N]^T$ and $\mathbf{g} = [g_1 \ g_2 \ g_3 \ \dots \ g_N]^T$ are arbitrary vector functions. This inner product allow us to introduce the adjoint variable of $\delta \mathbf{c}$, $\delta \mathbf{c}^+ = [\delta c_1^+ \ \delta c_2^+ \ \delta c_3^+ \ \dots \ \delta c_N^+]^T$, which satisfies the following relation:

$$\langle \mathbf{L} \delta \mathbf{c}, \delta \mathbf{c}^+ \rangle = \langle \delta \mathbf{c}, \mathbf{L}^+ \delta \mathbf{c}^+ \rangle + \mathbf{B}(\delta \mathbf{c}, \delta \mathbf{c}^+), \tag{11}$$

where

$$\mathbf{L}^+ = \begin{pmatrix} D \frac{\partial^2}{\partial x^2} + \alpha_1 & \beta_2 & 0 & \cdots & 0 \\ 0 & D \frac{\partial^2}{\partial x^2} + \alpha_2 & \beta_3 & \cdots & 0 \\ \vdots & \vdots & \ddots & \ddots & \vdots \\ 0 & 0 & \cdots & D \frac{\partial^2}{\partial x^2} + \alpha_{N-1} & \beta_N \\ 0 & 0 & \cdots & 0 & D \frac{\partial^2}{\partial x^2} + \alpha_N \end{pmatrix}, \quad (12)$$

and

$$\mathbf{B}(\delta \mathbf{c}, \delta \mathbf{c}^+) = D \sum_{n=1}^N \left(\delta c_n \frac{\partial \delta c_n^+}{\partial x} \Big|_{x=0} - \delta c_n \frac{\partial \delta c_n^+}{\partial x} \Big|_{x=L} \right) - D \delta c_1^+ \frac{\partial \delta c_1}{\partial x} \Big|_{x=0}. \quad (13)$$

Here, the right hand side is simply derived by performing integration by parts of the left hand side, and the boundary term $\mathbf{B}(c, \delta \mathbf{c}^+)$ stems from the unknown boundary values of $\delta \mathbf{c}^+$. Equation (8) allows us to rewrite Eq. (11) as:

$$\langle \delta \mathbf{p}, \delta \mathbf{c}^+ \rangle = -\langle \delta \mathbf{c}, \mathbf{L}^+ \delta \mathbf{c}^+ \rangle - \mathbf{B}(\delta \mathbf{c}, \delta \mathbf{c}^+). \quad (14)$$

We use a mathematical trick to extract the leading-order variation $\delta c_N|_{x=L}$. Note that the adjoint variable is not yet determined. By choosing the proper equation for the adjoint variable and its boundary condition, we can determine the leading-order variation $\delta c_N|_{x=L}$. We first set an equation for the adjoint variable $\delta \mathbf{c}^+$ as:

$$\mathbf{L}^+ \delta \mathbf{c}^+ = 0, \quad (15a)$$

and choose its boundary conditions as

$$\begin{aligned} D \frac{\partial \delta c_1^+}{\partial x} \Big|_{x=0} + \beta_1 \delta c_1^+ &= 0, & \frac{\partial \delta c_1^+}{\partial x} \Big|_{x=L} &= 0, \\ \frac{\partial \delta c_n^+}{\partial x} \Big|_{x=0} &= \frac{\partial \delta c_n^+}{\partial x} \Big|_{x=L} = 0, & \text{for } n &= 2, 3, \dots, N-1, \\ \frac{\partial \delta c_N^+}{\partial x} \Big|_{x=0} &= 0, & \frac{\partial \delta c_N^+}{\partial x} \Big|_{x=L} &= \frac{1}{D}, \end{aligned} \quad (15b)$$

resulting in the following relation:

$$\mathbf{B}(\delta \mathbf{c}, \delta \mathbf{c}^+) = -\delta c_N|_{x=L}. \quad (16)$$

Then, using Eqs. (14), (15a), and (16), we obtain the following relation for the leading-order variation of the final level of active protein concentration reaching the nucleus:

$$\delta c_N|_{x=L} = \langle \delta \mathbf{p}, \delta \mathbf{c}^+ \rangle. \quad (17)$$

Here, $\delta \mathbf{c}^+$ is now determined by(15a) and (15b).

From Eq. (5a), the leading-order variation $\delta c_N|_{x=L}$ can be written as:

$$\begin{aligned} \delta c_N|_{x=L} &= \sum_{n=1}^N \int_0^L \delta p_n \delta c_n^+ dx \\ &= \sum_{n=1}^N \left[\delta f_n \delta c_n^+(x_l) + \delta v_n^p(c_n(x_l)) \delta c_n^+(x_l) - \delta v_n^c(c_n(x_l)) \delta c_n^+(x_l) \right]. \end{aligned} \quad (18)$$

Here, the terms on the right hand side of Eq. (18) represent the effect of the release of active (phosphorylated) substrate protein ($\delta f_n \delta c_n^+$), kinase ($\delta v_n^p \delta c_n^+$), and phosphatase ($-\delta v_n^c \delta c_n^+$) on the concentration of phosphorylated protein at the nucleus ($c_N|_{x=L}$). Note that these terms are characteristic functions of the location x_l at which the source term $\delta p_n(x)$ is deployed: δc_n^+ , active substrate protein release; $\delta v_n^p \delta c_n^+ / \delta k_n^i$, kinase release; and $\delta v_n^c \delta c_n^+ / \delta k_n^a$, phosphatase release. These functions determine the leading-order variation in $\delta c_N|_{x=L}$, which implies that they represent the sensitivity of the target signal ($c_N|_{x=L}$) to the location at which the selected source term is positioned. Therefore, we will henceforth refer to these functions as the spatial sensitivities of the target signal to the release of phosphorylated substrate protein, kinase, and phosphatase, respectively. Finally, it should be noted that the leading-order variation is only a functional that consists of the unperturbed concentration (c_n) and the adjoint concentration (δc_n^+). Therefore, the leading-order variation is simply obtained by solving Eq. (4) with $\epsilon = 0$ along with Eq. (15).

2.3 Numerical methods

The steady solutions of Eqs. (4) and (7) are computed numerically. Spatial discretization is performed using the second-order central difference. The number of grid points is chosen as $N = 501$, sufficiently large to resolve all solutions. To reduce computational cost, steady solutions of Eqs. (4) and (15) are obtained using the Newton-Raphson iteration instead of a time-marching simulation. The code is implemented in Fortran 90. The baseline numerical solutions have been validated against those in Munoz-Garcia et al. (2009). All computations in this study were carried out on an Intel Xeon CPU E5345 operating Linux. The model parameters used in the present study is summarized in Table 1.

3 Results

3.1 Single protein modification cycle

Let us start by analyzing the simplest case, where the cascade consists of a single protein modification cycle ($N = 1$). We choose the spatial domain size as $L = 10 \mu\text{Pm}$, a representative size for many eukaryotic cells. For the diffusion coefficient and the deactivation rate by phosphatase, typical values are $D = 5 \times 10^{-12} \text{ m}^2 \text{ sec}^{-1}$

Table 1 Reaction constants in the present study

Parameters	Units	Reference value	Test range
k_1^a	m sec ⁻¹	5×10^{-6}	$5 \times 10^{-7} - 5 \times 10^{-2}$
k_n^a	sec ⁻¹	5	1.25 – 20
k_n^i	sec ⁻¹	5	Fixed
m_n^a	–	0.7	0.1 – 100
m_n^i	–	0.7	0.1 – 100

Here, k_n^a and k_n^i are the first-order rate constants for the linear kinetic domain respectively of the kinase and phosphatase reactions, and m_n^a and m_n^i are the dimensionless Michaelis constants. Note that k_1^a has different dimensions from other rate constants as it describes the reaction rate at the membrane. All the parameters given here are adopted from [Brown and Kholodenko \(1999\)](#), [Kholodenko \(2006\)](#), [Munoz-Garcia et al. \(2009\)](#)

and $k_1^i = 5 \text{ sec}^{-1}$ ([Kholodenko 2006](#)), which yield the characteristic length scale of the signal $\xi = 1 \text{ }\mu\text{m}$. For illustration purposes, we assume that the reaction is far from saturation: $m_n^a, m_n^i \gg 1$. If the reaction is far from saturation and for $\epsilon = 0$, Eqs. (4) and (15) can be solved analytically to yield:

$$c_1(x) = \frac{k_1^a}{k_1^a + \sqrt{k_1^i D}} \left(\frac{e^{-x/\xi} + e^{(x-2L)/\xi}}{1 + \eta e^{-2L/\xi}} \right), \tag{19}$$

where $\eta = (k_1^a - \sqrt{k_1^i D}) / (k_1^a + \sqrt{k_1^i D})$ and $\xi = \sqrt{D/k_1^i}$. Here, note that ξ is the length scale which characterizes how far the signal can be transmitted as discussed in the Introduction. Now, we consider the case of a non-zero ϵ so that the signal at the nucleus ($c_1(L)$) is modified due to the effect of $\epsilon \delta p_1(x)$. Thus, the signal c_1 is changed into $c_1 + \epsilon \delta c_1 + O(\epsilon^2)$. From Eq. (18), the leading-order variation δc_1 is given as follows:

$$\delta c_1|_{x=L} = \delta f_1 \delta c_1^+(x_l) + \delta k_1^a (1 - c_1(x_l)) \delta c_1^+(x_l) - \delta k_1^i c_1(x_l) \delta c_1^+(x_l), \tag{20}$$

where $\delta c_1^+(x_l)$, $(1 - c_1(x_l)) \delta c_1^+(x_l)$, and $-c_1(x_l) \delta c_1^+(x_l)$ are the spatial sensitivities of nuclear signaling to the release at $x = x_l$ of phosphorylated substrate protein, kinase, and phosphatase, respectively. The solution $\delta c_1^+(x)$ of the adjoint equation (20) is obtained as follows:

$$\delta c_1^+(x) = \frac{1}{\sqrt{k_1^i D}} \left(\frac{e^{(x-L)/\xi} - \eta e^{-(x+L)/\xi}}{1 + \eta e^{-2L/\xi}} \right). \tag{21}$$

Interestingly, the solution (21) of the adjoint equation also exhibits the same characteristic length scale ξ in its exponents, implying that this length scale also plays an important role in characterizing the spatial sensitivities of cellular signaling.

Fig. 2 Stationary concentration profiles of phosphorylated substrate proteins (a), and the corresponding spatial sensitivities to the release of (b) phosphorylated substrate protein, (c) kinase, and (d) phosphatase for a signaling cascade with a single protein modification cycle where the reaction is far from saturation ($m^a, m^t \gg 1$). The insets in panels (b) and (c) provide a zoom-in of the behavior near the cell membrane. Here, $k_1^a = 5 \times 10^{-7}, 5 \times 10^{-6}, 5 \times 10^{-5}, 5 \times 10^{-4}, 5 \times 10^{-2} \text{ m sec}^{-1}$

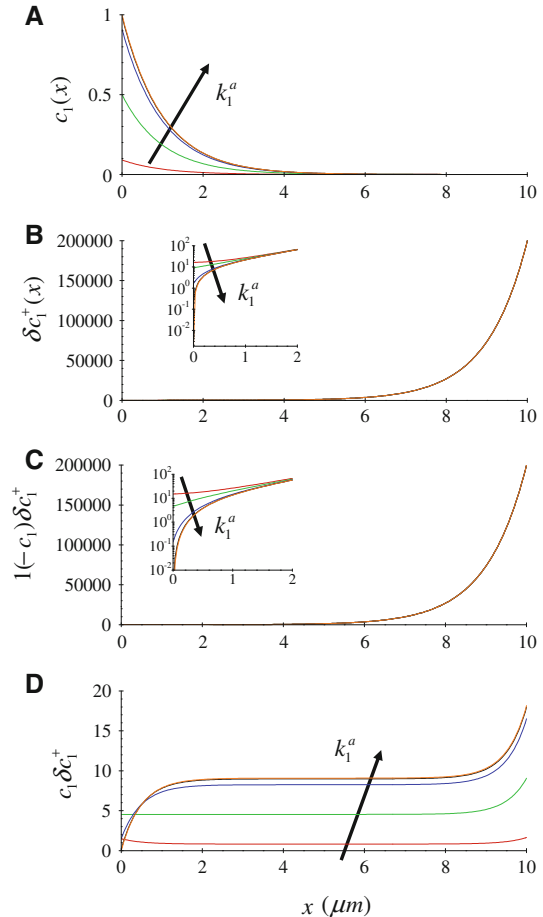


Figure 2a illustrates the steady-state spatial distribution of the phosphorylated substrate protein concentration for several activation rate constants at the cell membrane (k_1^a). The concentration is maximum at the cell membrane ($x = 0$) and minimum at the nucleus ($x = L$). As expected, the phosphorylated substrate protein concentration increases with increasing k_1^a throughout the spatial domain. This increase stops when the concentration at the cell membrane becomes saturated (i.e. $c_1|_{x=0} = 1$). For all k_1^a , the phosphorylated substrate protein concentration becomes quite low when the distance from the cell membrane exceeds the characteristic length scale (i.e. $x \in [\xi, L]$). This rapid drop leads to the formation of steep concentration gradients whose magnitude increases with k_1^a (Brown and Kholodenko 1999; Kholodenko 2002, 2006).

The spatial sensitivity to phosphorylated substrate protein release (δc_1^+) corresponding to the signal in Fig. 2a is depicted in Fig. 2b. For all k_1^a , the sensitivities increase rapidly with x in the vicinity of the nucleus and attain very large values at the nucleus. The sensitivity increase becomes particularly steep when the distance from the nucleus becomes smaller than the characteristic length scale ($x \in [L - \xi, L]$). This implies that

the release of phosphorylated substrate protein would be effective in regulating nuclear signaling only if the distance between the location of this release and the nucleus is smaller than the characteristic length scale ξ . Interestingly, the extent of this effectiveness appears to be virtually independent of signal intensity because changes in $\delta c_1^+(x)$ remain largely independent of k_1^a for most of the intracellular space. Only near the cell membrane does $\delta c_1^+(x)$ rapidly decay with an increase in k_1^a , probably due to the saturation of phosphorylated substrate protein concentration in that area (see inset of Fig. 2b).

Figure 2c shows the spatial sensitivity of nuclear signaling to kinase release ($(1 - c_1)\delta c_1^+$), which behaves very similar to the sensitivity to phosphorylated substrate protein release. This resemblance appears to originate from the nature of the kinase-mediated reaction: the kinase reaction rate is proportional to the unphosphorylated substrate protein concentration ($\bar{c}_1 (= 1 - c_1)$), and this value remains near saturation in most of the intracellular space away from the membrane as can be seen from Fig. 2a. Consequently, the spatial sensitivity to kinase release becomes virtually identical to that of phosphorylated substrate protein release in most of the intracellular space except near the membrane.

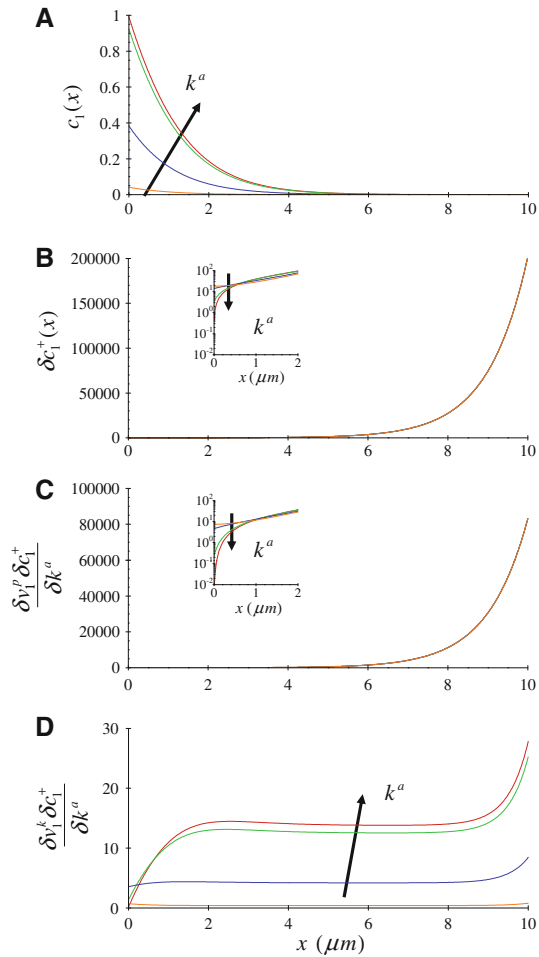
The spatial sensitivity of nuclear signaling to phosphatase release ($c_1\delta c_1^+$) is shown in Fig. 2d). Similar to the cases of phosphorylated substrate protein release and kinase release, the largest sensitivity is at the nucleus. Unlike the other cases, however, the sensitivity is relatively large even in the middle region of the cytoplasm. Furthermore, the dependence of the sensitivity on k_1^a is more pronounced for phosphatase release than for the other two cases. This very different behavior is attributable to the nature of the phosphatase-mediated reaction rate. This reaction is proportional to the phosphorylated substrate protein concentration; therefore, the sensitivity increases with an increase in k_1^a in most of the intracellular space. Near the membrane, however, the spatial sensitivity to phosphatase release decreases for sufficiently large k_1^a because the phosphorylation of the substrate protein can reach saturation in that region. Finally, it is interesting to note that the maximum of the spatial sensitivity to phosphatase is roughly two orders of magnitude smaller than that to kinase release. This implies that if kinase and phosphatase have nearly the same normalized rate constants, then regulation of nuclear signaling by phosphatase release would be much less effective than that achieved by kinase release.

Thus far, we have considered cases where the reaction is far from saturation ($m_1^a, m_1^i \gg 1$). However, we note that this assumption is not greatly limiting. In Fig. 3, we also examine the effect of saturation kinetics by numerically solving Eqs. (4) and (15) with physiological values of the non-dimensionalized Michaelis constants ($m_1^a = m_1^i = 0.7$). As clearly seen in this figure, the spatial sensitivities show no qualitative difference relative to the results in Fig. 2.

3.2 Cascade of multiple protein modification cycles

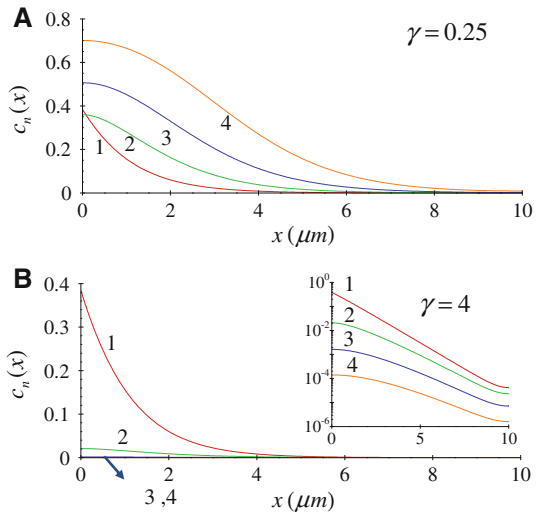
We now consider the more realistic situation where the cell signal is transmitted through a cascade of multiple protein modification cycles. For example, the ERK pathway consists of at least three protein modification cycles (Raf-Mek-ERK).

Fig. 3 Stationary (a) concentration profiles of phosphorylated substrate proteins, and the corresponding spatial sensitivities to (b) phosphorylated-substrate-proteins, c kinase, and (d) phosphatase release for the signal cascade with single protein-modification cycle where the reaction is set with physiological values of the normalized Michaelis constants ($m^a = m^i = 0.7$). Here, $k_1^a = 5 \times 10^{-7}, 5 \times 10^{-6}, 5 \times 10^{-5}, 5 \times 10^{-4}, 5 \times 10^{-2} \text{ m sec}^{-1}$



The presence of more levels in a cascade has often been thought to facilitate long-distance signal transfer (Brown and Kholodenko 1999; Kholodenko 2006). Therefore, in this section, we focus on how the nature of the cascade of multiple protein modification cycles modulates intracellular signal regulation. For illustration purposes, we consider a cascade of four protein modification cycles ($N = 4$). The spatial domain size is maintained the same as in the previous section (i.e. $L = 10 \mu\text{m}$). For simplicity, we assume that $k_n^i = k^i, m_n^a = m^a, m_n^i = m^i$ for all n and that $k_n^a = k^a$ for $n = 2, 3, 4$. Typical values are chosen for the rate constants of dephosphorylation and the dimensionless Michaelis constants following Brown and Kholodenko (1999); Kholodenko (2006); Munoz-Garcia et al. (2009): $k^i = 5 \text{ sec}^{-1}, m^a = m^i = 0.7$. Because we have already studied the effect of the rate constant at the cell membrane k_1^a (Fig. 2), a fixed value of this parameter is chosen: $k_1^a = 5 \times 10^{-6} \text{ m sec}^{-1}$. In signal cascades of multiple protein modification cycles, the phosphorylation and dephosphorylation rate constants k_a and k_i are crucial parameters in generating different signal propagation

Fig. 4 Stationary concentration profiles of phosphorylated substrate proteins in a signaling cascade ($N = 4$): **(a)** amplified case ($\gamma = 0.25$); **(b)** decaying case ($\gamma = 4$). The *inset* in panel **B** shows the behavior on a log plot to delineate the small differences near the cell membrane



patterns through the cascade. It has recently been proposed that the key parameter determining the nature of signal propagation through the cascade is the ratio between the dephosphorylation and phosphorylation rate constants in the linear kinetic domain (Munoz-Garcia et al. 2009):

$$\gamma \equiv \frac{k^i}{k_a} \tag{22}$$

The parameter γ plays an important role in determining to what extent an activated signal propagates through the cascade, i.e. whether it is amplified or decays as it travels through the cascade. The general relation of γ and the length of signals that travel through the cascade has been extensively discussed by Munoz-Garcia et al. (2009). In very large spatial domains, the amplification or decay of a cell signal propagating through the cascade is determined by a critical value γ_c (Munoz-Garcia et al. 2009). For $\gamma < \gamma_c$, signal transmission is promoted and the signal is amplified through each level of the cascade. On the other hand, for $\gamma > \gamma_c$, the signal experiences decay through each level of the cascade and thus becomes attenuated at the target location ($x = L$). In the present study, the rate constant of phosphorylation k_a at each level is varied in the range $k^a = 1.25 - 20 \text{ sec}^{-1}$, providing $\gamma = 0.25 - 4$. As we shall see later, γ_c is well within this range of γ .

We first compute solutions of Eq. (4) without any intracellular regulation (i.e. $\epsilon = 0$). Figure 4a, b show the resulting spatial concentration distributions of phosphorylated substrate proteins at each level of the cascade for $\gamma = 0.25$ and $\gamma = 4$, respectively. Similar to the case of a single-protein modification cycle (Figs. 2a, 3a), the phosphorylated substrate protein concentrations exhibit spatial gradients near the cell membrane at all cascade levels. The gradient at the cell membrane is steepest at the first level in the cascade ($n = 1$) and becomes progressively shallower in subsequent levels. For $\gamma = 0.25$, the concentration at a given intracellular location is amplified

Fig. 5 Stationary concentration of each level of phosphorylated substrate proteins at the nucleus with change of γ

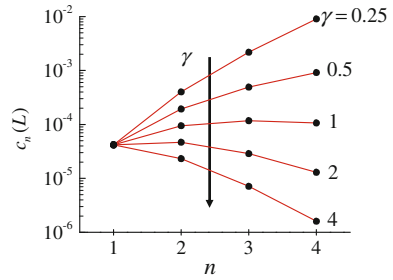
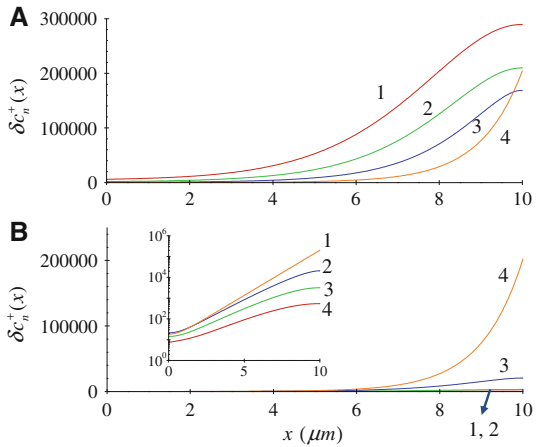


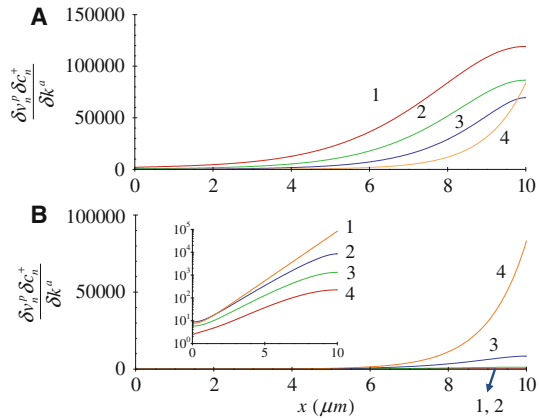
Fig. 6 Spatial sensitivity to phosphorylated substrate protein release in a signaling cascade: **a** amplified case ($\gamma = 0.25$); **b** decaying case ($\gamma = 4$). The inset in panel B shows the behavior on a log plot to delineate the small differences near the cell membrane



as the cascade level increases (Fig. 4a), indicating that the cascade promotes signal amplification. On the other hand, for $\gamma = 4$, the concentration decays very rapidly with cascade level (Fig. 4b). To determine an approximate value of γ_c in the present spatial domain ($L = 10 \mu\text{m}$), we examine several different γ values ($= 0.25, 0.5, 1, 2, 4$). Figure 5 demonstrates the dependence of the phosphorylated substrate protein concentration at the nucleus on the cascade level for the different γ values. For $\gamma \leq 0.5$, the phosphorylated substrate protein concentration at the nucleus increases with cascade level, implying that the signal is amplified by the cascade. On the other hand, for $\gamma > 1$, the concentration at the nucleus gradually decays as cascade level increases. These results suggest that $0.5 < \gamma_c < 1$ in the confined domain considered here, not too different from $\gamma_c \simeq 0.7$ obtained in unbounded spatial domains (Munoz-Garcia et al. 2009).

We next study the effect of adding intracellular signal regulation (i.e. incorporating the effect of δp_n in Eq. (5a)) by constructing the spatial sensitivities using the solution of the adjoint equation (15). The adjoint solution is obtained numerically using the same method as for the solution of the regular reaction-diffusion equation. Figure 6a and b depict the spatial sensitivities to phosphorylated substrate protein release for $\gamma = 0.25$ and $\gamma = 4$, respectively. For both cases, the spatial sensitivities at all levels in the cascade (δc_n^+) have their largest values at the nucleus, consistent with the results in the previous section (see Figs. 2b, 3b). For $\gamma = 0.25$, $\delta c_1^+ > \delta c_2^+ > \delta c_3^+ > \delta c_4^+$

Fig. 7 Spatial sensitivity to kinase release in a signaling cascade: **a** amplified case ($\gamma = 0.25$); **b** decaying case ($\gamma = 4$). The *inset* in panel **b** shows the behavior on a log plot to delineate the small differences near the cell membrane

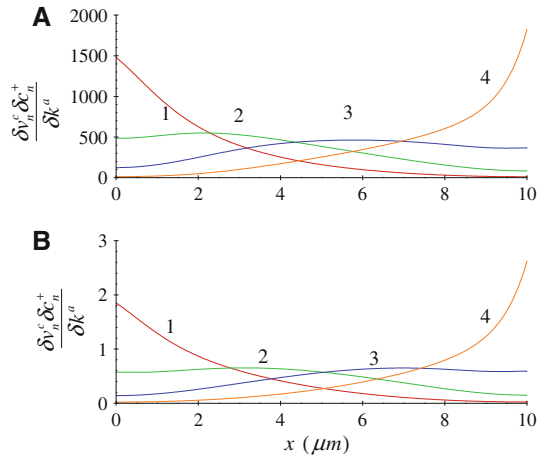


in most of the spatial domain (Fig. 6a), indicating that when the signal is amplified in propagating through the cascade ($\gamma < \gamma_c$), control of nuclear signaling by the release of phosphorylated substrate protein is more effective the further upstream in the cascade the release occurs. On the other hand, for $\gamma = 4$, $\delta c_1^+ < \delta c_2^+ < \delta c_3^+ < \delta c_4^+$ in most of spatial domain (Fig. 6b), leading to the opposite conclusion: release of phosphorylated substrate protein at the downstream end of the cascade is more effective than at the upstream end when the signal decays as it propagates through the cascade ($\gamma > \gamma_c$). Comparison of Fig. 6a and b indicates that the effect of γ on spatial sensitivity is largest for $n = 1$ and decreases progressively further downstream in the cascade. In fact, at the cascade level furthest downstream ($n = 4$), γ has no effect on the spatial sensitivity (δc_4^+ behavior is nearly identical in Fig. 6a, b). This finding suggests that if the intracellular signal is regulated via release of phosphorylated substrate protein, then the nature of signal propagation through the cascade (i.e. signal amplification vs. decay, which is determined by the value of γ) significantly affects the controllability of the signal at the nucleus.

Very similar behavior is observed for the spatial sensitivities to kinase release ($\delta v_n^p \delta c_n^+ / \delta k_n^a$) as seen in Fig. 7: the spatial sensitivities at all cascade levels have increase near the nucleus and attain their largest values at the nucleus. For $\gamma = 0.25$, the sensitivity increases progressively the farther upstream in the cascade the kinase is released (Fig. 7a), suggesting that control of signaling at the nucleus would be more effective by placing the kinase source at the upstream end of the cascade. In contrast, the kinase source would be more effectively positioned at the downstream end of the cascade for $\gamma = 4$ (Fig. 7b). As in the single protein cycle case (see Figs. 2, 3), the structural similarity between the dependence of spatial sensitivities on kinase release and on phosphorylated substrate protein release stems from the nature of the kinase-mediated reaction, which is proportional to the concentration of unphosphorylated substrate proteins ($\bar{c}_n(1 - c_n)$).

Finally, the spatial sensitivities to phosphatase release ($\delta v_n^c \delta c_n^+ / \delta k_n^i$) are presented in Fig. 8 for $\gamma = 0.25$ and $\gamma = 4$. As in the case of the single protein modification cycle (cf. Figs. 2, 3), the spatial sensitivities to phosphatase release show significantly different behavior from those to phosphorylated substrate protein release or

Fig. 8 Spatial sensitivity to phosphatase release in a signaling cascade: **a** amplified case ($\gamma = 0.25$); **b** decaying case ($\gamma = 4$)



kinase release. At all cascade levels, the sensitivities to phosphatase release are fairly uniformly distributed throughout the cytoplasm, unlike the cases of phosphorylated substrate protein release and kinase release where the sensitivities are clearly highest near the nucleus. As already described, this feature originates from the nature of the phosphatase-mediated reaction, which is proportional to the concentration of phosphorylated substrate proteins. For phosphatase release, the sensitivities exhibit very different spatial distributions depending on the level within the signaling cascade. For $n = 1$, the maximum sensitivity is at the cell membrane. As the cascade level n increases, the location of the maximum sensitivity gradually moves towards the nucleus and is at the nucleus for the last level of the cascade ($n = 4$). This implies that the most effective spatial location for phosphatase release within the cytoplasm depends on the cascade level at which this release occurs. Contrary to the cases of phosphorylated proteins and kinase release, γ appears to affect signal regulation by intracellular phosphatase release almost uniformly at all cascade levels: an increase in γ significantly lowers sensitivities for all cascade levels (Fig. 8a, b). The shapes of the spatial sensitivity curves, however, are largely independent of γ (compare Fig. 8a, b).

In an earlier section, we had investigated the effect of γ on signal amplification and decay (cf: Fig. 5). To further explore the ramifications of this aspect of signal propagation, we studied the effect of γ on the sensitivity of the signal at either the cell membrane or the nucleus to the release of phosphorylated substrate protein, kinase, or phosphatase at the different levels in the signaling cascade (Fig. 9). At both the cell membrane and the nucleus, the sensitivities to phosphorylated substrate protein release and to kinase release for small γ ($\gamma < 0.5$) are largest at the most upstream level of the cascade ($n = 1$) (Fig. 9a–d). Increasing γ markedly reduces these sensitivities except for the case of the most downstream level of the cascade ($n = 4$) where the sensitivities become independent of γ . These findings suggest that for $\gamma > 1.0$, release of phosphorylated substrate protein and/or kinase in the upstream levels of the cascade is ineffective for controlling the signal at either the cell membrane or

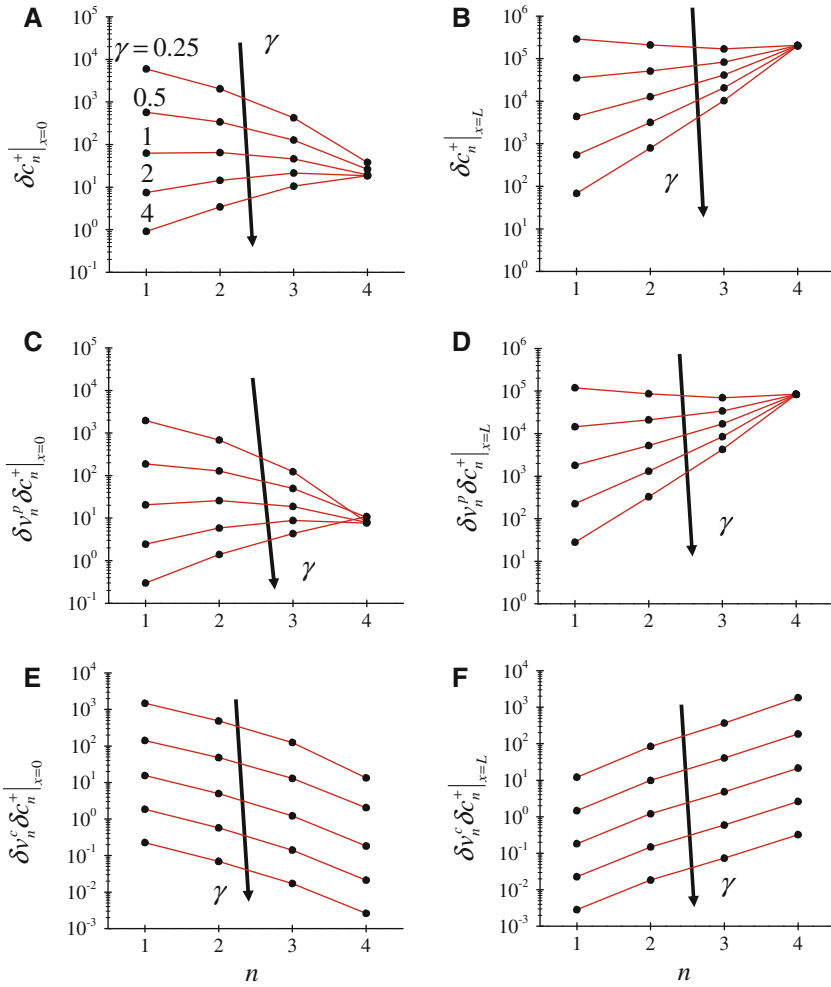


Fig. 9 Dependence on γ of the spatial sensitivities to (a, b) phosphorylated substrate protein release, (c, d) kinase release, (e, f) phosphatase release in each level of a signaling cascade: (a, c, e) cell membrane ($x = 0$); (b, d, f) nucleus ($x = L$)

the nucleus. The sensitivities to phosphatase release behave quite differently from the sensitivities to phosphorylated substrate protein release or kinase release (Fig. 9e, f). At the cell membrane, the maximum sensitivity is obtained at the farthest upstream level of the cascade ($n = 1$) (Fig. 9e), whereas at the nucleus, the most downstream levels of the cascade ($n = 4$) exhibits the maximum sensitivity (Fig. 9f). Contrary to the sensitivities to phosphorylated substrate protein release and kinase release, an increase in γ results in an almost uniform decrease in the sensitivities to phosphatase release at all cascade levels (Fig. 9e, f). This behavior is probably attributable to the nature of the phosphatase-mediated reaction.

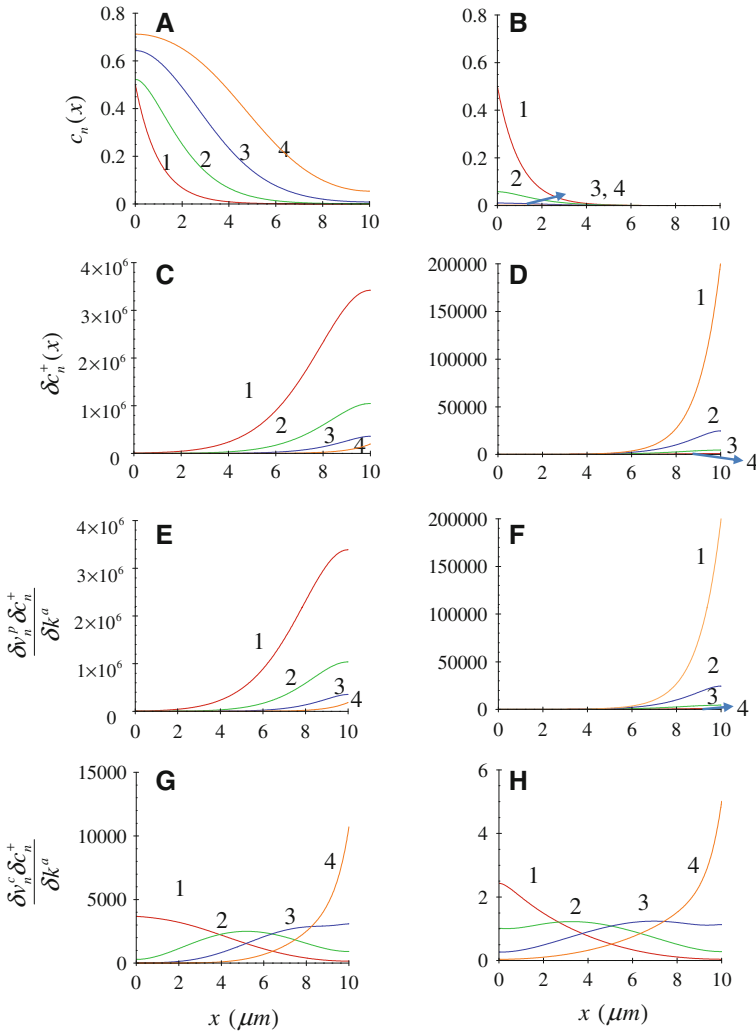


Fig. 10 Effect of the Michaelis constants ($m^a = 100, m^i = 100$): **a, b** concentration profiles of phosphorylated substrate proteins; the corresponding spatial sensitivities to (**c, d**) phosphorylated-substrate-proteins, (**e, f**) kinase, and (**g, h**) phosphatase release for the signal cascade of four protein-modification cycles. Here, (**a, c, e, g**) propagating ($\gamma = 0.25$) and (**b, d, f, h**) decaying ($\gamma = 4$) signals through the cascade

We note that structure and behavior of the spatial sensitivities with γ do not significantly depend on the changes in the Michaelis constants. In Figs. 10, 11, and 12, we examined different values of the Michaelis constants. Consistent with observation in signaling with single protein modification cycle (see the Sect. 3.1), the spatial sensitivities to phosphorylated substrate protein, kinase, and phosphatase release with different Michaelis constants reveal qualitatively the same behavior with those with the physiological values of the Michaelis constants ($m^a = m^i = 0.7$).

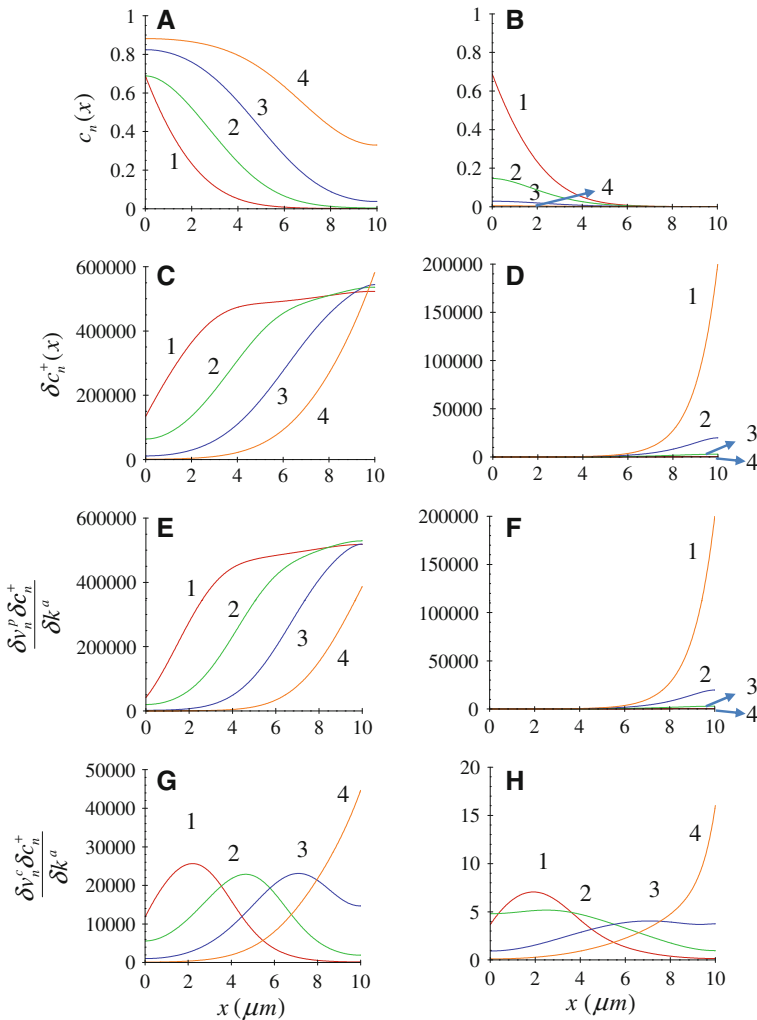


Fig. 11 Effect of the Michaelis constants ($m^a = 100, m^i = 0.1$): **a, b** concentration profiles of phosphorylated substrate proteins; the corresponding spatial sensitivities to **(c, d)** phosphorylated-substrate-proteins, **(e, f)** kinase, and **(g, h)** phosphatase release for the signal cascade of four protein-modification cycles. Here, **(a, c, e, g)** propagating ($\gamma = 1$) and **(b, d, f, h)** decaying ($\gamma = 5$) signals through the cascade

4 Discussion

4.1 How location makes a difference

In this paper, we have used variational analysis to study the sensitivity of signaling in protein modification cycles to spatial variations in the localized release of phosphorylated substrate protein, kinase, and phosphatase. The results indicate that for the release of substrate protein and/or kinase, signal regulation is effective only if the

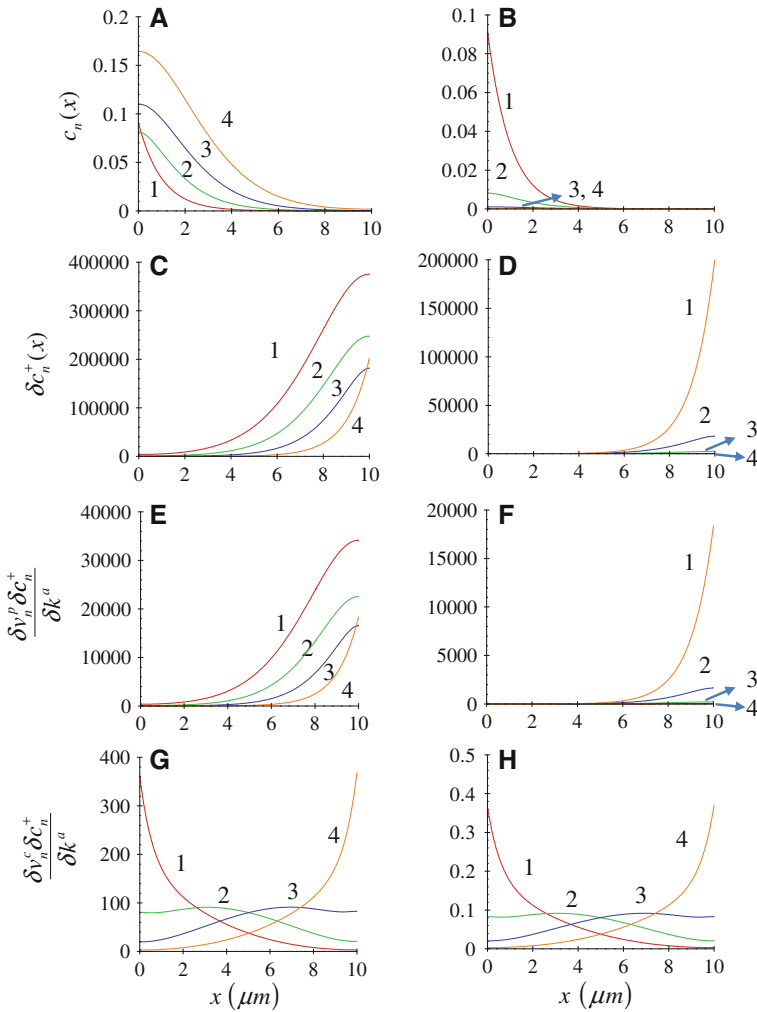


Fig. 12 Effect of the Michaelis constants ($m^a = 0.1, m^i = 100$): **a, b** concentration profiles of phosphorylated substrate proteins; the corresponding spatial sensitivities to **(c, d)** phosphorylated-substrate-proteins, **(e, f)** kinase, and **(g, h)** phosphatase release for the signal cascade of four protein-modification cycles. Here, **(a, c, e, g)** propagating ($\gamma = 0.05$) and **(b, d, f, h)** decaying ($\gamma = 0.5$) signals through the cascade

distance between the localized release source and the target (d_{target}) is sufficiently small. A simple dimensional analysis provides interesting additional insight into this notion. If we consider a signaling complex which releases phosphorylated substrate protein and/or kinase, then the signal provided by this complex and which originates at the cell membrane would be transmitted over a distance of $O(\xi)$ only because of limitations on transport due to the presence of phosphatase in the cytoplasm. Therefore, signal regulation by this complex would only be effective if the target is located within a distance $O(\xi)$:

$$d_{\text{target}} \lesssim O(\xi). \quad (23)$$

This explains why the adjoint solution also yields the same length scale as the original reaction-diffusion equation. Using typical values, $\xi = 1 \mu\text{m}$ while cell size is $O(10) \mu\text{m}$, which suggests that signal regulation at the nucleus would only be effective if intracellular complexes intended to mediate this regulation are positioned sufficiently closely to the nucleus. This is consistent with the observation that many intracellular signaling complexes such as endosomes, lysosomes and the Golgi apparatus are localized preferentially around the nucleus (Burkhardt et al. 1997; Harada et al. 1998).

For a signaling complex that releases or acts as a phosphatase, the range of its effectiveness in signal regulation would be determined by a competition between the distance from the source over which significant phosphatase activity persists and the length scale given by Eq. (23). Because the phosphatase reaction rate is proportional to the concentration of phosphorylated substrate protein and because this concentration is expected to be largest near the cell membrane, reaction associated with phosphatase-releasing signaling complexes would be most active around the cell membrane. However, this location is far from the target location (the nucleus) which, in accordance with Eq. (23), would render signal regulation by this complex quite ineffective. Placing the signaling complex near the nucleus does not resolve the dilemma because the concentration of phosphorylated protein in that region is lower than that near the cell membrane, which would reduce phosphatase reaction rate and hence the effectiveness of the signaling complex. These arguments lead to the conclusion that signal regulation at the nucleus by a phosphatase source would be largely ineffective regardless of where this source is positioned within the intracellular space. This conclusion is broadly supported by the present numerical results (see Figs. 2, 3, 8, 9).

Finally, we should stress that the spatial preference of the intracellular regulation discussed here has been found to be robust to the choice of dimensionless Michaelis constants, which directly controls ultrasensitivity and bistability of the reactions in the present system (see Figs. 10, 11, 12). It has recently been shown that the presence of space in the MAPK pathway leads to loss of ultrasensitivity and bistability (Takahashi et al. 2010). However, the robustness of the present findings to the nature of ultrasensitivity and/or bistability suggests that the spatial preference of the intracellular regulation discussed here would not be changed as long as the formation mechanism of the spatial gradient of phosphorylated substrate protein is preserved.

4.2 Importance of the nature of the signaling cascade

The analysis of the cascade with multiple protein modification cycles has demonstrated that the effectiveness of signal regulation at the nucleus is also strongly dependent on the nature of signal propagation through the cascade. If the intracellular signal is amplified as it propagates through the cascade, then most of reactions in the cascade exhibit high sensitivity to release from localized signaling complexes. In particular, for regulation by release of phosphorylated signal proteins and/or kinase, reactions in the upstream levels of the cascade exhibit particularly high sensitivities. On the

other hand, if the intracellular signal decays as it propagates through the cascade, then the reactions in the cascade generally lose their ability to effectively control cell signaling, and reactions in upstream levels of the cascade become considerably less effective than those in the downstream levels. Importantly, these results appear to be a general feature, as they are also observed for different reaction constants and diffusion coefficients (see Figs. 10, 11, 12).

Protein modification cycle cascades are thought of as a mechanism for effective signal transmission to distant intracellular target sites via signal amplification (Brown and Kholodenko 1999; Kholodenko 2006). Within this context, the present analysis suggests that localized release of factors that modulate the reactions within protein modification cycles provides an effective tool for robust intracellular signaling regulation. Importantly, regulation by the release of phosphorylated substrate protein and/or kinase becomes very effective particularly for the upstream reactions in the cascade (Fig. 9a–d). This might explain why membrane receptors, which primarily drive reactions near the cell membrane, are so effective in regulating intracellular signaling.

4.3 Application to endocytosis: a model analysis

As a specific example of the application of the present analysis, we focus on endosome-mediated intracellular signal regulation. It should be noted in this regard that the model depicted in Fig. 1 is considerably simpler than the actual physiological situation. Furthermore, the present analysis neglects temporal dynamics, which play an important role in cellular signal transduction. Therefore, the analysis presented here is valid only in a qualitative sense for most of the signaling cascades which exhibits rich spatio-temporal dynamics. However, we note that the steady analysis here may also be relevant to some specific cases such as MAPK response to NGF (nerve growth factor) stimulation which exhibits sustained behavior for hours (Marshall 1995; Wu et al. 2001) (see also discussion in Sect. 4.4). We consider a signaling cascade identical to the one discussed in the previous section. For simplicity, the parameter values for reaction constants and diffusion coefficient are assumed to be the same as those in the previous section, and a signal that gets amplified as it propagates through the cascade ($\gamma = 0.25$) is considered to mimic the physiologically relevant situation. We assume that the cell membrane loses its signaling complexes due to internalization of receptors during endocytosis and that the internalized signaling complexes are transported by vesicles to an endosome located at $x = x_e$. Since our approach is limited to the steady case ($\partial/\partial t = 0$), the movement of the vesicles and the endosome are neglected. Finally, we assume that the internalized membrane signaling complexes phosphorylate signaling proteins for the reaction at the most upstream level of the cascade (i.e. $n = 1$) in a similar way as those at the cell membrane. Thus, these assumptions allow us to describe endosome-mediated intracellular signal regulation $\epsilon\delta p_n$ as follows:

$$\epsilon\delta p_n = \epsilon\delta_{n1} \left[\frac{k_1^a(1 - c_1)}{1 + (1 - c_1)/m_1^a} \delta(x - x_e) - \frac{k_1^a(1 - c_1)}{1 + (1 - c_1)/m_1^a} \delta(x) \right], \quad (24)$$

where δ_{n1} is the Kronecker delta function. Here, the first term on the right hand side describes the phosphorylation rate of substrate proteins by the internalized signaling complexes in the endosome, while the second term represents the reduced phosphorylation activity at the cell membrane due to the internalization of the signaling complexes. For illustration purposes, we choose $\epsilon = 0.1$, implying that 10 % of signaling complexes at the cell membrane are transported to the endosome. Then, from Eq. (18), the leading-order change of $c_4|_{x=L}$ due to this type of intracellular signal regulation is given by

$$\epsilon \delta c_4|_{x=L} = \epsilon \left[\frac{k_1^a(1-c_1)}{1+(1-c_1)/m_1^a} \delta c_1^+(x_e) - \frac{k_1^a(1-c_1)}{1+(1-c_1)/m_1^a} \delta c_1^+(0) \right]. \quad (25)$$

Note that $\epsilon \delta c_4|_{x=L}$ now appears as only a function of the location of endosome x_e .

Figure 13 shows the leading-order change of the most downstream signal reaching the nucleus as a function of the location of the endosome. To understand the effect of cell size, two different sizes of the intracellular domain, $L = 10 \mu\text{m}$ and $L = 100 \mu\text{m}$, are considered as shown in Fig. 13a, b, respectively. For both cases, the leading-order change of the target signal ($\epsilon \delta c_4|_{x=L}$) by the modeled endosome becomes significant when the endosome is located near the nucleus. Interestingly, the maximum amount of signal regulation, which is obtained at the nucleus, is almost identical in the two cases, suggesting that the maximum ability of signal regulation does not depend on cell size if the endosome is positioned properly within the intracellular space (near the nucleus in this case). Cell size matters, however, in the sense that for small cells ($L = 10 \mu\text{m}$), the endosome is effective to some extent even in the middle of the spatial domain ($x = 5 \mu\text{m}$): the regulation effect at $x = 5 \mu\text{m}$ is about 20 % of the maximum that can be obtained at the nucleus (Fig. 13a). In contrast, for large cells ($L = 100 \mu\text{m}$), an endosome positioned in the middle of the spatial domain ($x = 50 \mu\text{m}$) has little influence on the signal reaching the nucleus (Fig. 13b), implying that the endosome would be ineffective in most of the intracellular space except in the close vicinity of the nucleus. It has been suggested the endosome plays no role in long-distance signal transduction in large cells (Birtwistle and Kholodenko 2009). The present result suggests that if the endosome is positioned sufficiently close to the nucleus, then endocytosis may indeed play an important role in signal regulation even for a very large cell.

For both small and large cells, the effect of the endosome decays exponentially as its distance from the nucleus increases. Consequently, for endosomes located near the cell membrane, their effect on signaling is expected to be negligible even if they function normally in activating cell signals. This finding is consistent with recent experimental results that have demonstrated that displacing endosomes to the vicinity of the cell membrane significantly disturbs MAPK signaling (Taub et al. 2007). It is of course recognized that the function of endosomes and related signaling cascades are much more complicated than those described here (Flore and Camilli 2001; Kholodenko 2002, 2003; Perlson et al. 2005; Miaczynska et al. 2004; Howe and Mobley 2004; Birtwistle and Kholodenko 2009); however, the present analysis may provide a conceptual rationale for why endosomes localize preferentially near the nucleus.

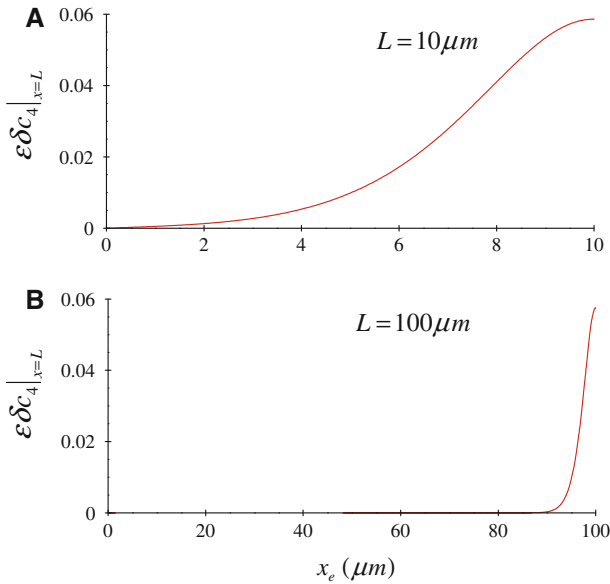


Fig. 13 The leading-order variation of the most downstream phosphorylated substrate at the nucleus with respect to the change in the location of the modeled endosome x_e

Finally, one may consider the fact that real organelles have finite sizes. In the present one-dimensional model, it may be relevant to consider two point sources instead of one point source as in Eq. (24): for example,

$$\epsilon \delta p_n = \epsilon \delta_{n1} \left[\frac{k_1^a(1-c_1)/2}{1+(1-c_1)/m_1^a} \delta(x-x_e+r) + \frac{k_1^a(1-c_1)/2}{1+(1-c_1)/m_1^a} \delta(x-x_e-r) - \frac{k_1^a(1-c_1)}{1+(1-c_1)/m_1^a} \delta(x) \right], \tag{26}$$

where r is the radius of the given organelle. We note that Eq. (26) becomes identical to Eq. (24) as $r \rightarrow 0$. Using Eq. (18), it is straightforward to obtain the leading-order variation of the most downstream signal reaching the nucleus as follows:

$$\epsilon \delta c_4|_{x=L} = \epsilon \delta_{n1} \left[\frac{k_1^a(1-c_1)/2}{1+(1-c_1)/m_1^a} \delta c_1^+(x_e-r) + \frac{k_1^a(1-c_1)/2}{1+(1-c_1)/m_1^a} \delta c_1^+(x_e+r) - \frac{k_1^a(1-c_1)}{1+(1-c_1)/m_1^a} \delta c_1^+(0) \right]. \tag{27}$$

Since $r \ll L$ in many cases, the dependence of the leading-order variation $\epsilon \delta c_4|_{x=L}$ on the location of the organelle x_e from the two-points model (26) would be very similar to that shown in Fig. 13. However, we should point out that the two-point model clearly exhibits the effect of the organelle's size. For instance, when the organelle is bound to the cell membrane ($x_e = r$), $\epsilon \delta c_4|_{x=L}$ is not strictly zero unlike in the case of

the one-point model (24) (see also Fig. 13). On the other hand, when the organelle is bound to the nucleus ($x_e = L - r$), the amount of signal upregulation from the two-point model becomes smaller than that from the one-point model.

4.4 Limitations and outlook

Probably the most important contribution of the present work is the quantification using variational analysis of the role of space in intracellular signaling regulation for given models of signaling cascades. For example, the role of endocytosis discussed here has been analyzed by a few recent studies (Kholodenko 2002, 2006; Birtwistle and Kholodenko 2009) in which similar mathematical models are directly solved with the driving term provided at a fixed location (typically midpoint between signal source and target). In the present study, we show that applying the variational approach to those models greatly simplifies their analysis because the solution of the adjoint equation enables us to visualize the full information on the role of 'space' in endocytosis-mediated cell signaling. This suggests that the variational analysis introduced here could be potentially extended to more realistic models and provide much deeper understanding of the role of intracellular signaling complexes in cell signaling cascades.

Although the variational analysis in the present study is limited to the steady case, it still provides useful physical insights into the role of intracellular signaling regulation for some specific cases. One of the well-known examples is cell signaling outcome of the PC12 cell-line stimulation with NGF. PC12 cells exhibit sustained MAPK response for hours after treatment with NGF (Marshall 1995), and the current steady analysis would probably be directly applicable to this case. Indeed, it has been experimentally shown that disturbing endosomes and the Golgi apparatus inhibits the sustained MAPK response with NGF stimulation (Wu et al. 2001), consistent with the analysis in Sect. 4.3.

However, it should be pointed out that in many cases, cell signaling often exhibits much richer spatio-temporal patterns than the simply sustained response due to the fact that the architecture of signaling cascades in many cells is much more complicated than the simple top-down signaling cascade assumed here (see Fig. 1). For example, in MAP kinase signaling driven by EGF (epidermal growth factor), negative signal feedback from ERK to Raf is present, which essentially generates temporally transient ERK activation (Brightman and Fell 2000). The presence of such feedback or feedforward loops in signaling cascades is expected to lead to considerably richer spatio-temporal dynamics (Tyson et al. 2003; Kholodenko 2006). Indeed, it has recently been shown that bistability in signaling cascades triggers traveling waves which propagate from the cell membrane to the nucleus with near constant speed (Markevich et al. 2006; Munoz-Garcia et al. 2010; Zhao et al. 2011). Furthermore, signaling activation at upstream could also be dependent in time as cells often experience change in their environment (Zhao et al. 2011). From this perspective, a natural follow-up would be to apply the variational analysis to spatio-temporally dynamic signaling cascades. This can be done by extending the present inner product space (Eq. 10), taking only space into account, to time domain. We expect that this extension would provide sensitivity information of given signaling patterns in both time and space, and understanding its spatio-temporal

correlation to the given signaling patterns would enable us to access much richer information on the role of intracellular regulation in cell signaling cascades. We believe that this analysis would become an useful framework to enhance our understanding of signaling cascades as well as cellular physiology.

Acknowledgments This work was funded in part by an endowment in Cardiovascular Cellular Engineering from the AXA Research Fund.

Appendix: Normalization of the model

The reaction-diffusion equations for the signaling cascade in Fig. 1 are given as follows (Munoz-Garcia et al. 2009):

$$\begin{aligned} \frac{\partial C_1}{\partial t} &= D \frac{\partial^2 C_1}{\partial x^2} - V_1^{phos} + \epsilon \delta P_1(x, t), \\ \frac{\partial C_n}{\partial t} &= D \frac{\partial^2 C_n}{\partial x^2} + V_n^{kin} - V_n^{phos} + \epsilon \delta P_n(x, t) \quad \text{for } n = 2, 3, \dots, N \end{aligned} \tag{28a}$$

with boundary conditions,

$$\begin{aligned} D \frac{\partial C_1}{\partial x} \Big|_{x=0} &= -V_1^{kin}, \quad \frac{\partial C_1}{\partial x} \Big|_{x=L} = 0, \\ \frac{\partial C_n}{\partial x} \Big|_{x=0} &= \frac{\partial C_n}{\partial x} \Big|_{x=L} = 0 \quad \text{for } n = 2, 3, \dots, N, \end{aligned} \tag{28b}$$

where the reaction terms are given as

$$\begin{aligned} V_1^{kin} &= V_{max,1}^{kin} \frac{C_1^{tot} - C_1}{K_1^{kin} + C_1^{tot} - C_1} \Big|_{x=0}, \\ V_n^{kin} &= k_{cat,n}^{kin} \frac{C_{n-1}(C_n^{tot} - C_n)}{K_n^{kin} + C_n^{tot} - C_n} \quad \text{for } n = 2, 3, \dots, N, \\ V_n^{phos} &= V_{max,n}^{phos} \frac{C_n}{K_n^{phos} + C_n} \quad \text{for } n = 1, 2, \dots, N. \end{aligned} \tag{29}$$

Here, $k_{cat,n}^{kin}$ is the catalytic constant (turnover number), $V_{max,1}^{kin}$ the maximal rate for the kinase at the cell membrane, $V_{max,n}^{phos}$ the maximal rate for the phosphatase at level n of the cascade, K_n^{kin} the Michaelis constant for the kinase at level n , and K_n^{phos} the Michaelis constant for the phosphatase at level n . Normalization of Eq. (1) by C_{1tot} leads to the normalized reaction terms as in Eq. (4), where $v_n^{kin} = V_1^{kin} / C_{1tot}$ and $v_n^{phos} = V_n^{phos} / C_{1tot}$ for all n . The apparent first-order rate constants in Eq. (4) are

readily obtained as:

$$k_1^a = \frac{V_{max,1}^{kin}}{K_1^{kin}}, \quad k_n^a = \frac{k_{cat,n}^{kin} C_{n-1}^{tot}}{K_n^{kin}} \quad \text{for } n = 2, 3, \dots, N, \quad (30)$$

$$k_n^i = \frac{V_{max,n}^{phos}}{K_n^{phos}} \quad \text{for } n = 1, 2, 3, \dots, N.$$

Similarly, the normalized (dimensionless) Michaelis constants in Eq. (4) are given as:

$$m_n^a = \frac{K_n^{kin}}{C_{tot}^{tot}}, \quad m_n^i = \frac{K_n^{phos}}{C_{tot}^{tot}} \quad \text{for } n = 1, 2, 3, \dots, N. \quad (31)$$

References

- Asthaigiri AR, Lauffenburger DA (2001) A computational study of feedback effects on signal dynamics in a mitogen-activated protein kinase (mapk) pathway model. *Biotechnol Prog* 17:227–239
- Bhalla US, Ram PT, Iyengar R (2002) Map kinase phosphatase as a locus of flexibility in a mitogen-activated protein kinase signaling network. *Science* 297:1018–1023
- Birtwistle MR, Kholodenko BN (2009) Endocytosis and signalling: a meeting with mathematics. *Mol Oncol* 3:308–320
- Bivona TG, de Castro IP, Ahearn IM, Grana TM, Chiu VK, Lockyer PJ, Cullen PJ, Pellicer A, Cox AD, Philips MR (2003) Phospholipase c-gamma activates ras on the golgi apparatus by means of rasgrp1. *Nature* 424:694–698
- Brightman FA, Fell DA (2000) Differential feedback regulation of the mapk cascade underlies the quantitative differences in egf and ngf signaling in pc12 cells. *FEBS Lett* 482:169–174
- Brown GC, Kholodenko BN (1999) Spatial gradients of cellular phospho-proteins. *FEBS Lett*. 457:452–454
- Burkhardt JK, Echeverri CJ, Nilsson T, Vallee RB (1997) Over-expression of the dunamitin (p50) subunit of the dynein complex disrupts dynein-dependent maintenance of membrane organelle distribution. *J Cell Bio* 139:469–484
- Chang L, Karin M (2001) Mammalian map kinase signaling cascades. *Nature* 410:37–40
- Ferrell JE (1997) How responses get more switch-like as you move down a protein kinase cascade. *Trends Biochem Sci* 78:288–289
- Flore PPD, Camilli PD (2001) Endocytosis and signaling: an inseparable partnership. *Cell* 106:1–4
- Goldbeter A, Koshland DE (1981) An amplified sensitivity arising from covalent modification in biological systems. *Proc Natl Acad Sci* 78:6840–6844
- Gunzburger MD (2003) Perspectives in flow control and optimization. SIAM, Philadelphia
- Harada A, Takei Y, Kanai Y, Tanaka Y, Nanoka S, Hirokawa N (1998) Golgi vesiculation and lysosome dispersion in cells lacking cytoplasmic dynein. *J Cell Bio* 141:51–59
- Hoepfner S, Severin F, Cabezas A, Habermann B, Runge A, Gillyooly D, Stenmark H, Zerial M (2005) Modulation of receptor recycling and degradation by the endosomal kinesin kif216b. *Cell* 121:437–450
- Howe CL, Mobley WC (2004) Signaling endosome hypothesis: a cellular mechanism for long distance communication. *J Neurobiol* 58:207–216
- Kalab P, Weis K, Heald R (2002) Visualization of a ran-gtp gradient in interphase and mitotic xenopus egg extracts. *Science* 295:2452–2456
- Kholodenko BN (2002) Map kinase cascade signalling and endocytic trafficking: a marriage of convenience? *Trends Cell Biol*. 12:173–177
- Kholodenko BN (2003) Four-dimensional organization of protein kinase signaling cascades: the roles of diffusion, endocytosis and molecular motors. *J Exp Biol* 206:2073–2082
- Kholodenko BN (2006) Cell-signaling dynamics in time and space. *Nat Rev Mol Cell Biol* 7:165–176
- Kholodenko BN (2010) Signaling ballet in space and time. *Nat Rev Mol Cell Biol* 7:165–176
- Koenig JA, Edwardson JM (1997) Endocytosis and recycling of g protein-coupled receptors. *Trends Pharmacol Sci* 18:276–287

- Maeder CI, Hink MA, Kinkhabwala A, Mayr R, Bastiaens PI (2007) Spatial regulation of *fos3* map kinase activity through a reaction-diffusion mechanism in yeast pheromone signaling. *Nat Cell Biol* 9:1319–1326
- Markevich NI, Tsyganov MA, Hoek JB, Kholodenko BN (2006) Long-range signaling by phosphoprotein waves arising from bistability in protein kinase cascades. *Mol Sys Biol* 2:61
- Marshall CJ (1995) Specificity of receptor tyrosine kinase signaling: transient versus sustained extracellular signal-regulated kinase activation. *Cell* 80:179–185
- Miaczynska M, Pelkmans L, Zerial M (2004) Not just a sink: endosomes in control of signal transduction. *Curr Opin Cell Biol* 16:400–406
- Munoz-Garcia J, Neufeld Z, Kholodenko BN (2009) Positional information generated by spatially distributed signaling cascades. *Plos Comp Biol* 5(3):e100330
- Munoz-Garcia J, Neufeld Z, Kholodenko BN (2010) Signaling over a distance: gradient patterns and phosphorylation waves within single cells. *Biochem Soc Trans* 38(5):1231–1241
- Nakayama K, Satoh T, Igari A, Kageyama R, Nishida E (2008) Fgf induces oscillations of *hes1* expression and *ras/erk* activation. *Curr Biol* 18:R332–334
- Niethammer P, Bastiaens P, Karsenti E (2004) Stathmin-tubulin interaction gradient in motile and mitotic cells. *Science* 303:1862–1866
- Perlson E, Hanz S, Ben-Yaakov K, Segal-Ruder Y, Seger R, Fainzilber M (2005) Vimentin-dependent spatial translocation of an activated map kinase in injured nerve. *Neuron* 45:715–726
- Pierce KL, Maudsley S, Daaka Y, Luttrell LM, Lefkowitz RJ (2000) Role of endocytosis in the activation of the extracellular signal-regulated kinase cascade by sequestering and nonsequestering g protein-coupled receptors. *Proc Natl Acad Sci* 97(4):1489–1494
- Sadowski L, Pilecka I, Miaczynska M (2009) Signaling from endosomes: location makes a difference. *Exp Cell Res* 315:1601–1609
- Stadtman ER, Chock PB (1977) Superiority of interconvertible enzyme cascades in metabolic regulation: analysis of monocyclic systems. *Proc Natl Acad Sci* 74:2761–2765
- Stelling J, Kholodenko BN (2009) Signaling cascades as cellular devices for spatial computations. *J Math Biol* 58:35–55
- Takahashi K, Tanase-Nicola S, ten Wolde PR (2010) Spatio-temporal correlations can drastically change the response of a mapk pathway. *Proc Natl Acad Sci USA* 107(6):2473–2478
- Takai L, Sasaki T, Matuzaki T (2001) Small gtp-binding proteins. *Physiol Rev* 81:153–208
- Taub N, Teis D, Ebner HL, Hess MW, Huber LA (2007) Late endosomal traffic of the epidermal growth factor receptor ensures spatial and temporal fidelity of mitogen-activated protein kinase signaling. *Mol Biol Cell* 18(12):4698–4710
- Tyson JJ, Chen KC, Novak B (2003) Sniffers, buzzers, toggles and blinkers: dynamics of regulatory and signaling pathways in the cell. *Curr Opin Cell Biol* 15:221–231
- Warren DT, Tajsic T, Mellad JA, Searles R, Zhang Q, Shanahan CM (2010) Novel nuclear nesprin-2 variant tether active extracellular signal-regulated mapk1 and mapk2 at promyelocytic leukemia protein nuclear bodies and act to regulate smooth muscle cell proliferation. *Nat Rev Mol Cell Bio* 10:75–82
- Wu C, Lai CF, Mobley WC (2001) Nerve growth factor activates persistent rap1 signaling in endosomes. *J Neurosci* 21(15):5406–5416
- Xiong W, Ferrell JE (2003) A positive-feedback-based bistable ‘memory module’ that governs a cell fate decision. *Nature* 426:460–465
- Zhao Q, Yi M, Liu Y (2011) Spatial distribution and dose-response relationship for different operation modes in a reaction-diffusion model of the mapk cascade. *Phys Biol* 8:055004